Hindawi
Mathematical Problems in Engineering
Volume 2019, Article ID 4691641, 17 pages
https://doi.org/10.1155/2019/4691641

Research Article

Dynamic Spreading Model of Passenger Group Panic considering Official Guidance Information in Subway Emergencies

Jiayang Li,[1,2] **Jiafu Tang**,[3] **and Dan Wang**[2]

[1]*School of Business Administration Northeastern University, Shenyang, Liaoning 110000, China*
[2]*School of Information Engineering Shenyang University, Shenyang, Liaoning 110044, China*
[3]*School of Management Science and Engineering Dongbei University of Finance and Economics, Dalian, Liaoning 116025, China*

Correspondence should be addressed to Jiayang Li; jiayang_neu@163.com

Received 21 July 2019; Accepted 26 September 2019; Published 23 October 2019

Academic Editor: Gisele Mophou

Safety concerns are increasing as rail transportation develops at a fast pace. When emergencies erupt in the course of transportation, panic will spread among passengers. Subway operators should understand how the emotions of passengers spread and how the guidance instructions work, in order to effectively deter the transmission of panic. Based on the models of system dynamics, transmission dynamics, and contagious disease, the essay constructs a dynamic transmission model for passenger panic inside the carriage, incorporating the official guidance instructions. Then, the essay utilizes Routh–Hurwitz criteria and analyzes the stability equilibrium of the dynamic differential equation. Mathematical analysis and simulation tests have verified the validity of the model and stability conditions. Finally, it is proved in the essay by mathematical analysis and simulation tests that official guidance instructions can effectively control the spread of panic and quickly stabilize the system. Thus, the essay helps subway operators to come up with clear official guidance, so as to find quick solutions and prevent escalation of panic due to lack of trust.

1. Introduction

With the growth of population and the acceleration of urbanization, subway is becoming the public's first choice to transport passengers due to the advantages of large volume, fast speed, and convenience [1]. Since the 1970s, subway stations around the world have seen frequent security incidents, such as terrorist bombings, riots, crowds, and stampedes [2]. However, due to the high population density of the subway and the small enclosed space, panic caused by emergencies can spread rapidly [3]. In serious cases, traffic accidents occur in chaos, which will further aggravate the impact of the whole event. In such an emergency, if evacuees can calm the panic as soon as possible, casualties can be avoided or significantly reduced [4]. Therefore, proper official guidance can save many lives in an emergency. Therefore, the preparation of evacuation guidance is of great significance to pedestrian evacuation. Evacuation leaders can improve the efficiency of crowd evacuation when evacuees are not familiar with evacuation routes. The allocation of leaders' numbers and positions is particularly important for the efficiency of evacuation [5]. So, we think, the official manager of subway operation will release the guidance information in time and maintain the authenticity and credibility of the guidance information, which plays an important role in controlling passengers' panic.

When abnormal events break out in the subway operation, the normal safe environment is broken, and subway passengers will be nervous. Tension will expand, when psychological tension reaches a certain level, and it will cause psychological panic, its internal performance, namely, panic mood. Earlier studies have shown that in the face of terrible disasters, people will lose their basic humanity and fall into the fear of beasts [6]. As for the panic among subway passengers, scholars have done the following research studies. Mawson [7] pointed out that the panic comes from

awareness and has relationship with social organization, culture, environment, situational factors, and social control. Ebihara et al. [8] analyzed the behavior of individual panic. Low [9] believes that in the context of relatively spontaneous behavior and disorder, the unconscious spread of emotions of each participant in the group, causing group behavior. Aguirre [10] clarified that panic can be described as psychological panic and panic behavior. The causes of group panic are analyzed, which are influenced by the closeness of group members, the kinship of group participants, the external environment, and the information of events.

In recent years, scholars have done these research studies on subway passengers' panic and group evacuation. Wang et al. [11] conducted a simulation experiment of emergency evacuation at Junbo station of Beijing subway line 1. A model for estimating the panic degree of people in emergency evacuation of subway was established. The results show that the degree of panic in the process of emergency evacuation of subway is influenced by individual differences such as age, quantity of articles, safety education level, and relevant accident experience, as well as by environmental factors such as personnel density, complexity of evacuation environment, and accident location. Yu et al. [12] proposed the evacuation entropy particle swarm optimization (e-pso) model, verifying that individual panic will aggravate the chaos of events, but adding guidance will reduce the chaos and improve the efficiency of evacuation. Yu et al. [13] analyzed the causes and features of emergencies in subway or railway station through empirical research, including fire, terrorist attack, flood, earthquake, stampede, and other accidents. Eren Başak et al. [14] used emotional infection model and crowd to simulate three events, such as bombing attack, subway panic, and Black Friday peak, and optimized the emotional characteristic parameters of actors from the data extracted from the video segment of the event. Yang [15] conducted complex modeling on the scale of subway passengers in large cities in China, analyzed the safety problems caused by a large number of passenger flows, and summarized and proposed preventive and coping measures on large-scale passenger flows. Liang et al. [16] used 24 models to analyze the causes of unsafe behaviors and habitual behaviors in the metro fire accident in Daegu, South Korea, and discussed people's unsafe behaviors and unsafe psychological state in the subway fire. Wang et al. [17], based on KAP theory, established the structural equation model of nonadaptive behavior of subway evacuation passengers. The influence of passengers' internal knowledge and safety risk awareness on escaping from danger is analyzed. Wang et al. [18] established a dynamic evacuation risk analysis model considering psychological and behavioral responses of evacuees by using event tree analysis (ETA). Hong et al. [19] used the principle of ripple effect to simulate the dissemination and acquisition of information in panic, and at the same time, considered the self-organization of group behavior and modeled the phenomenon of passengers' self-evacuation in the emergency of subway station. Zhang et al. [20] improved an ASET/RSET method. Taking an actual subway station in the Wuhan subway system as an example, considering the characteristics of fire, buildings, and people, Mao et al. modeled the phenomenon of passengers' self-evacuation in subway station emergencies. Mao et al. [21] adopted the Marine personality model and OCC emotional model to propose an emotion-based diversified behavior model on the basis of introducing the CA–SIRS emotional infection model. Psychology-based individual modeling enables our model to be applied to a variety of scenarios.

In the subway emergency safety guidance strategy, Li's [22] survey on the perspective of urban administration showed that the traffic flow between the subway exit and the business district was very dense. The results of the survey helped managers to control crowds and riots on the spot [5]. Sun et al. [23] studied the subway station entrance before adding funnel bottleneck buffer, through the walking speed, individual through time and total, through the analysis of the factors such as time and time interval, and found that the funnel shape overall improves the transportation efficiency of neck, for organizations in the bottleneck, to improve existing pedestrian traffic efficiency and provide a theoretical basis. Li et al. [24] explored the three shortest ways for passengers to get to the exit in the subway station in Taipei, Taiwan, no map is needed, aided by 2D and 3D maps. The results show that the design of underground space map should support certain direction and floor wayfinding strategy, and select the appropriate perspective. Huang et al. [25] believed that when there were obstacles in the evacuation node, the overall evacuation ability of fire would be seriously affected. By simulating the existence of obstacles in the typical subway station fire evacuation simulation node, the results show that the flow rate, evacuation time, and obstacle of evacuation node affect the safe evacuation ability. Song et al. [26] adopted the FDS + EVAC simulation method to study the fire evacuation time of subway trains with high passenger flow density by analyzing the concentration of harmful gas and temperature distribution of smoke. Cao et al. [27] studied the pedestrian evacuation with guidance with a multigrid model and discussed the type of guidance strategy, the number and distribution of guidance personnel, and the influence of different guidance strategies on evacuation.

In the research of emotional transmission mechanism, this paper is based on information transmission dynamics and epidemiology. Liu et al. [28] established a nonlinear mathematical model for information dissemination of public emergencies and studied the information dissemination mechanism of online social networks. Through the accurate estimation of information dissemination of public emergencies, a new method of information dissemination of public emergencies is proposed. Xu et al. [29] proposed and studied a new SIVRS mathematical model for the spread of infectious diseases. The optimal control strategies of susceptible agents, infectious agents, and mutants were studied by considering the mutation factors in the transmission of virus in complex networks. Zhang et al. [30] studied the diffusion effect environment of information in coupled

social networks, and used two new node states to enhance information transmission. Using the improved SIR model, the simulation results of integrated data show that the environment of coupled social network influences the information diffusion, so the information diffusion has a long relaxation time node. Huo et al. [31] believed that rumors caused unnecessary conflicts and confusion by misleading the public, and their propagation had a great impact on human affairs. Rumors and suspicions often stem from a lack of official information. Taking the scientific education process in which officials repeatedly deny rumors as the periodic impulse as the research object, researchers proposed a rumor propagation model with pulse inoculation and time delay, and analyzed the global dynamic behavior of officials repeatedly denying rumors. Li et al. [32] proposed a systematic model to describe the spread of deep anemia in the country of Cote d'Ivoire, which combines factors such as human mobility, the intensity of human interaction, and demographic characteristics. Kan and Zhang [33] studied the spread of infectious diseases and the interplay of human activity as consciousness spreads through multiple networks. In the model, it is an infectious disease. Whether it can be spread in one network, representing the path of infectious disease transmission, and lead to the spread of consciousness in information networks. Then, the spread of consciousness causes individuals to adopt social distance, which affects the spread of epidemic diseases. Zhu and Wang [34] proposed an improved SIR model to study the spread of rumors in complex social networks and deduced a stochastic differential equation (SDE) to characterize the diffusion dynamics of rumors in homogeneous and heterogeneous networks. Then, through the theoretical analysis of uniform network, the solution of SDE model and the steady state of rumor diffusion are studied. Zang [35] proposed a global consciousness control communication model (GACS), in which individuals are easily influenced by global consciousness information considering the existence of group behavior. By using the global microscopic Markov chain method, the analysis result of epidemic threshold value is obtained. Jiang and Yan [36] built a new online social network (OSN) model of susceptibility—infection—elimination (SIR) rumor propagation. The stability analysis of the model shows that communicators in social networks have a basic reproduction number. Meanwhile, a control method of rumor propagation based on the SIR model of immune structure is proposed. The stability analysis and numerical simulation of the model suggest that immunization of susceptible population is an effective method to control rumor propagation.

As mentioned above, in the current research, when subway emergencies are involved, passenger emotions are mainly studied in qualitative and empirical aspects. However, quantitative analysis of passenger sentiment is rare. In many literatures, passenger emotions often appear as a factor of evacuation strategy in the form of a certain parameter. However, we believe that the formation mechanism of the emotional transmission of subway passengers is from individual emotions to mass panic. In particular, there are fewer literatures analyzing the relationship between official guidance information and passenger panic, and most papers focus on the implementation of guidance strategies.

This paper, combining system dynamics, epidemiology, and information transmission dynamics, constructs a subway passenger panic mode with official guidance information and tries to analyze the evolution mechanism of passenger panic and the control effect of official guidance information on passenger panic. The main contents are as follows. Section 2 builds the passenger panic propagation model with guiding information in subway emergency based on system dynamics and transmission dynamic. Section 3 analyses theoretical analysis of equilibrium stability using Routh–Hurwitz criteria. In Section 4, a dynamic panic propagation model of subway passengers with guidance strategies is established, and the stability of dynamic system is analyzed and verified by the numerical method. At last, Section 5 pointed out the research significance of this paper and the next research direction.

2. The Passenger Panic Propagation Model with Guiding Information in Subway Emergencies

2.1. The Definition of the Passenger Groups. In the process of subway operations, passengers will panic when abnormal events occur. The panic will spread further if there is no effective guiding strategy. This paper establishes a passenger panic propagation model that considers the participation of official guidance strategies. On this basis, we can analyze the formation mechanism of panic and the degree of influence of the official guidance strategy on panic control.

In this paper, passengers in subway cars are mainly divided into three states according to their own degree of panic. The susceptible group (S) easily changes states and becomes infected. The infected group (I) spreads panic to the surrounding passengers. The calm group (R) is similar to the immune population in SIRS, but they can also be affected by internal and external causes.

When an actual emergency occurs, the composition of the different states and their changes are as follows.

2.1.1. Susceptible Group (S). When an emergency occurs, passengers are not immediately aware of its severity, so the majority of the passengers are nervous but do not panic. With the increased information transmission during the outbreak of a crisis, passengers have more details about what happened. Passengers change states depending on the environmental and psychological factors along with time t.

The susceptible group is affected by the surrounding infected group. A certain proportion is then infected and becomes part of the infected group. At the same time, some passengers will gradually calm down due to receiving and following the official guidance information, which directly moves them into the calm group.

2.1.2. Infected Group (I). When a crisis breaks out, part of the reason for this is because of people's own nervousness. Fear can spread and affect the susceptible group. As time passes, the panicked group becomes calm due to the decrease of their panic, their increased familiarity with their external environment, and their decreased fear of danger. In addition, they may accept the official guidance information and be influenced by other reasons.

2.1.3. Calm Group (R). During the outbreak of a crisis, the mood of the crowd will change, so we believe that there is no calm group at the start. As t passes, the calm group is separated from the potential group and the panicked group. At the same time, the calm group is unstable, and its members change their status due to internal and external factors. The internal cause is the loss of trust in the guiding information. For example, as time passes and the event is not addressed, the crowd will become restless and agitated. At this time, the trust in the official guiding information will decrease, leading to the transformation of the calm group into the susceptible group. The external reason is that if the number of people around the panic is very large, calm passengers will also be affected and will gradually become not calm.

2.2. Dynamic SIRS Model and Parameters. There are many factors influencing emotional transmissions in emergencies. In this paper, the passenger panic propagation model with guidance information is discussed with the following assumptions:

(1) There are three types of people in the system: the susceptible group, the infected group, and the calm group. At time t, the ratio of each group to the total population is, respectively, expressed as $S(t)$, $I(t)$, and $R(t)$. In the initial state, there is only the susceptible group and infected group, and the proportion of the potential group is larger than that of the panicked group. There is no calm group when $t = 0$, which means that $R(0) = 0$.

(2) According to Article 37 of the Urban Rail Transit Engineering Project Construction Standards 104-2008 of the Ministry of Housing and Urban-Rural Development, the evaluation standard for the density of standing passengers in a vehicle is 3 persons per square meter for comfort, 4 or 5 persons per square meter for good, and 6 persons per square meter for dense. Therefore, it is considered in this paper that the personnel density $\widehat{k} = 2.5$ is in line with the comfort standard of off-peak and uncrowded subway operations.

(3) In cases of emergencies, the condition is considered that the subway car does not arrive at the station or stops suddenly without opening the door. In the process of emotional transmission $S(t) + I(t) + R(t) = 1$, which means that there is no change in the number of people.

Based on system dynamics and transmission dynamics, this paper establishes an improved dynamic differential equation of the SIRS infectious disease model by using formulas (1)–(3), which are used to describe and model the evolution of passengers' panic in subway cars with guidance information when a sudden crisis takes place. Its parameters and state transformation relations are shown in Figure 1.

$$\frac{\mathrm{d}S(t)}{\mathrm{d}t} = -\alpha\widehat{k}I(t)S(t) + \gamma\widehat{k}I(t)R(t) + \widetilde{\lambda}_3 R(t) - \lambda_1 S(t), \tag{1}$$

$$\frac{\mathrm{d}I(t)}{\mathrm{d}t} = \alpha\widehat{k}I(t)S(t) - \beta\widehat{k}I(t)R(t) - (\varepsilon + \lambda_2)I(t), \tag{2}$$

$$\frac{\mathrm{d}R(t)}{\mathrm{d}t} = \beta\widehat{k}I(t)R(t) + (\varepsilon + \lambda_2)I(t) + \lambda_1 S(t) - \gamma\widehat{k}I(t)R(t) - \widetilde{\lambda}_3 R(t). \tag{3}$$

We assume that α is the infected rate and describes the probability of infection in a potential population if an uninfected person contacts an infected person. β is the calm-infected rate, which is the recovery rate when affected by the calm group. When the surrounding environment is calm, then there will be less fear among infected persons since the surrounding groups are all calm groups. Parameter β indicates the probability that the panic-infected person will gradually calm down if the calm group appears around the infected person. γ is the immune loss rate and shows the ratio of the calm group to the susceptible group when the calm person contacts the infected group during time t. ε represents the recovery rate and is used to describe the probability of self-recovery of infected people when their own panic decreases. In an emergency environment, infected people are a nervous group, so the index value is not too large.

This paper focuses on the impact of guidance information on the spread of panic among passengers. Therefore, three parameters are used to describe the attitudes of different groups to official guidance. λ_1 represents the rate of susceptibility to infected passengers with guidance. Considering that the emergency broke out in a subway car, this value represents the proportion of the susceptible group who had accepted the evacuation control strategy, followed the guidance, and turned into calm people. λ_2 is the conversion rate of infected to recovery with guidance. In an emergency, this value is the percentage of infected people who were calm because they accepted the evacuation control strategies and followed instructions. $\widetilde{\lambda}_3$ represents the guidance loss rate of recovery. In emergency situations, calm people usually have a high degree of trust in official guidance messages. Nevertheless, as the situation worsens or as time passes and the danger does not abate, the calm person's dependence on guidance will gradually decrease. At this point, even the calm people have the potential to become infected, which increases the instability of the system and the variety of the states.

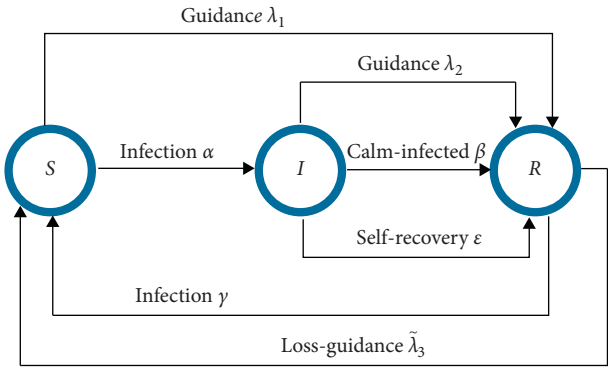

FIGURE 1: The evolutionary model of passengers' panic in subway cars with guidance.

3. Theoretical Analysis of Equilibrium Stability

Considering the occurrence of abnormal events during subway operations, the dynamic diffusion model of group panic with guidance is shown in equations (1) and (2). Regardless of whether passengers get on or off, the total number of people in the compartment is constant. The number of people in the car is N, and $S(t) + I(t) + R(t) = 1$. The model can be expressed by two differential equations as follows:

$$\frac{dS(t)}{dt} = -\alpha\hat{k}I(t)S(t) + \gamma\hat{k}I(t)[1 - I(t) - S(t)] + \tilde{\lambda}_3[1 - I(t) - S(t)] - \lambda_1 S(t), \tag{4}$$

$$\frac{dI(t)}{dt} = \alpha\hat{k}I(t)S(t) - \beta\hat{k}I(t)[1 - I(t) - S(t)] - (\varepsilon + \lambda_2)I(t). \tag{5}$$

Using the Routh–Hurwitz criteria, the asymptotic stability of the equilibrium for equations (4) and (5) is calculated. We can also use the Jacobian matrix of equations (4) and (5) to illustrate this as follows:

$$J = \begin{pmatrix} -\lambda_1 - \tilde{\lambda}_3 - \alpha\hat{k}I(t) - \gamma\hat{k}I(t) & -\tilde{\lambda}_3 - \gamma\hat{k}[I(t) + S(t) - 1] - \alpha\hat{k}S(t) - \gamma\hat{k}I(t) \\ \alpha\hat{k}I(t) + \beta\hat{k}I(t) & \beta\hat{k}[2I(t) + S(t) - 1] + \alpha\hat{k}S(t) - \lambda_2 - \varepsilon \end{pmatrix}. \tag{6}$$

Theorem 1. *When* $0 < \alpha\hat{k}/(\varepsilon + \lambda_2) < 1$, $E_1 = (S^*, I^*) = (1, 0)$ *is one disease-free equilibrium for equations (4) and (5).*

Proof. Assumption:

$$\frac{dS}{dt} = f(S), \tag{7}$$

and we construct $H(S, S^*) = f(S) - f'(S) \cdot (S - S^*)$.

The basic conditions for the Routh–Hurwitz criteria are shown by

$$H(S^*, S^*) = 0,$$
$$\lim_{S \longrightarrow S^*} \frac{|H(S, S^*)|}{|S - S^*|} = 0. \tag{8}$$

Because

$$H(S^*, S^*) = f(S^*) - f'(S) \cdot (S^* - S^*) = 0,$$
$$\lim_{S \longrightarrow S^*} \frac{|H(S, S^*)|}{|S - S^*|} = \lim_{S \longrightarrow S^*} \frac{|f(S) - f'(S) \cdot (S - S^*)|}{|S - S^*|} = 0. \tag{9}$$

Therefore, equations (4) and (5) satisfy the basic conditions of the Routh–Hurwitz criteria.

Equation (6) of the Jacobian matrix at the rumor-free equilibrium $E_1 = (S^*, I^*) = (1, 0)$ can be written as follows:

$$J_1 = \begin{pmatrix} -\lambda_1 - \tilde{\lambda}_3 & -\alpha\hat{k} - \tilde{\lambda}_3 \\ 0 & \alpha\hat{k} - \varepsilon - \lambda_2 \end{pmatrix}. \tag{10}$$

We describe the characteristic equation of matrix J_1 as

$$\det(J_1 - \mu E) = \begin{vmatrix} -\lambda_1 - \tilde{\lambda}_3 - \mu & -\alpha\hat{k} - \tilde{\lambda}_3 \\ 0 & \alpha\hat{k} - \varepsilon - \lambda_2 - \mu \end{vmatrix} = \mu^2 + \left[\left(\lambda_1 + \tilde{\lambda}_3\right) - \alpha\hat{k} - \varepsilon - \lambda_2\right]\mu - \left(\lambda_1 + \tilde{\lambda}_3\right)\left(\alpha\hat{k} - \varepsilon - \lambda_2\right). \tag{11}$$

Set $a_1 = (\lambda_1 + \tilde{\lambda}_3) - (\alpha\hat{k} - \lambda_2 - \varepsilon)$ and $a_2 = -(\lambda_1 + \tilde{\lambda}_3) \cdot (\alpha\hat{k} - \lambda_2 - \varepsilon)$.

If $0 < \alpha\hat{k}/(\varepsilon + \lambda_2) < 1$, $a_1 > 0$, and $a_2 > 0$ based on the Routh–Hurwitz criteria, the equilibrium point E_1 is asymptotically stable if $0 < \alpha\hat{k}/(\varepsilon + \lambda_2) < 1$. □

Theorem 2. *When* $\alpha\hat{k}/(\varepsilon + \lambda_2) > 1$ *and* $0 < (((\alpha + \beta)\hat{k})/(\beta\hat{k} + \varepsilon + \lambda_2)) < 1$, $E_2 = (S^*, I^*) = (\tilde{\lambda}_3/(\lambda_1 + \tilde{\lambda}_3), 0)$ *is the other disease-free equilibrium for the differential model made of equations (4) and (5).*

Proof. Equation (6) for the Jacobian matrix at the rumor-free equilibrium $E_2 = (S^*, I^*) = (\tilde{\lambda}_3/(\lambda_1 + \tilde{\lambda}_3), 0)$ can be written as

$$J_2 = \begin{pmatrix} -\lambda_1 - \tilde{\lambda}_3 & -\alpha\hat{k}S(t) - \tilde{\lambda}_3 + \gamma\hat{k}[1 - S(t)] \\ 0 & \beta\hat{k}[S(t) - 1] + \alpha\hat{k}S(t) - \varepsilon - \lambda_2 \end{pmatrix}. \tag{12}$$

We describe the characteristic equation of matrix J_2 as

$$\begin{aligned}
\det(J_2-\mu E) &= \begin{vmatrix} -\lambda_1-\widetilde{\lambda}_3-\mu & -\alpha\widehat{k}S(t)-\widetilde{\lambda}_3+\gamma\widehat{k}[1-S(t)] \\ 0 & \beta\widehat{k}(S(t)-1)+\alpha\widehat{k}S(t)-\varepsilon-\lambda_2-\mu \end{vmatrix} \\
&= \mu^2+\Delta_1\mu+\Delta_2, \\
\therefore 0 &< \frac{(\alpha+\beta)\widehat{k}\cdot\widetilde{\lambda}_3}{\left(\beta\widehat{k}+\varepsilon+\lambda_2\right)\cdot\left(\lambda_1+\widetilde{\lambda}_3\right)} < 1, \\
\Delta_1 &= \left(\lambda_1+\widetilde{\lambda}_3\right)-\left\{(\alpha+\beta)\widehat{k}\cdot\left[\frac{\widetilde{\lambda}_3}{\left(\lambda_1+\widetilde{\lambda}_3\right)}\right]-\left(\beta\widehat{k}+\lambda_2+\varepsilon\right)\right\} \\
&> \left(\lambda_1+\widetilde{\lambda}_3\right) \\
&> 0, \\
\Delta_2 &= -\left(\lambda_1+\widetilde{\lambda}_3\right)\cdot\left\{(\alpha+\beta)\widehat{k}\cdot\left[\frac{\widetilde{\lambda}_3}{\left(\lambda_1+\widetilde{\lambda}_3\right)}\right]-\left(\beta\widehat{k}+\lambda_2+\varepsilon\right)\right\} \\
&= -(\alpha+\beta)\widehat{k}\widetilde{\lambda}_3+\frac{\left(\beta\widehat{k}+\lambda_2+\varepsilon\right)}{\left(\lambda_1+\widetilde{\lambda}_3\right)} \\
&> -(\alpha+\beta)\widehat{k}\widetilde{\lambda}_3+(\alpha+\beta)\widehat{k}\widetilde{\lambda}_3 \\
&> 0,
\end{aligned} \tag{13}$$

therefore, $0 < (((\alpha+\beta)\widehat{k}\cdot\widetilde{\lambda}_3)/((\beta\widehat{k}+\varepsilon+\lambda_2)\cdot(\lambda_1+\widetilde{\lambda}_3))) < 1$, $\Delta_1 > 0$, and $\Delta_2 > 0$ based on the Routh–Hurwitz criteria. Thus, the model, based on equations (4) and (5), has an equilibrium point E_2 that is asymptotically stable. □

Theorem 3. *When* $\alpha\widehat{k}/(\varepsilon+\lambda_2) > 1$, $(((\alpha+\beta)\widehat{k})/(\beta\widehat{k}+\varepsilon+\lambda_2)) > 1$ *and* $(((2\beta-\alpha-\gamma)\widehat{k}I^*+(\alpha+\beta)\widehat{k}S^*)/(\beta\widehat{k}+\lambda_1+\lambda_2+\widetilde{\lambda}_3+\varepsilon)) < 1$, $E_3 = (S^*, I^*)$, $S^* \neq 0$ *and* $I^* \neq 0$ *is the one and only endemic equilibrium point.*

Proof. The Jacobian matrix is converted to equation (14) by substituting $E_3 = (S^*, I^*)$ into equation (6)'s Jacobian matrix.

$$J_3 = \begin{pmatrix} -\lambda_1-\widetilde{\lambda}_3-\alpha\widehat{k}I^*-\gamma\widehat{k}I^* & -\widetilde{\lambda}_3-\gamma\widehat{k}(I^*+S^*-1)-\alpha\widehat{k}S^*-\gamma\widehat{k}I^* \\ \alpha\widehat{k}I^*+\beta\widehat{k}I^* & \beta\widehat{k}(2I^*+S^*-1)+\alpha\widehat{k}S^*-\lambda_2-\varepsilon \end{pmatrix}. \tag{14}$$

We describe the characteristic equation of matrix J_3 as

$$\begin{aligned}
\det(J_3-\mu E) &= \begin{vmatrix} -\lambda_1-\widetilde{\lambda}_3-\alpha\widehat{k}I^*-\gamma\widehat{k}I^*-\mu & -\widetilde{\lambda}_3-\gamma\widehat{k}(I^*+S^*-1)-\alpha\widehat{k}S^*-\gamma\widehat{k}I^* \\ \alpha\widehat{k}I^*+\beta\widehat{k}I^* & \beta\widehat{k}(2I^*+S^*-1)+\alpha\widehat{k}S^*-\lambda_2-\varepsilon-\mu \end{vmatrix} \\
&= \mu^2+c_1\mu+c_2.
\end{aligned} \tag{15}$$

Set

$$\begin{aligned}
c_1 &= \left(\lambda_1+\widetilde{\lambda}_3+\alpha\widehat{k}I^*+\gamma\widehat{k}I^*\right)-\left[\beta\widehat{k}(2I^*+S^*-1)+\alpha\widehat{k}S^*-\lambda_2-\varepsilon\right], \\
c_2 &= -\left(\lambda_1+\widetilde{\lambda}_3+\alpha\widehat{k}I^*+\gamma\widehat{k}I^*\right)\cdot\left(\beta\widehat{k}(2I^*+S^*-1)+\alpha\widehat{k}S^*-\lambda_2-\varepsilon\right) \\
&\quad -\left(\alpha\widehat{k}I^*+\beta\widehat{k}I^*\right)\cdot\left[-\widetilde{\lambda}_3-\gamma\widehat{k}(I^*+S^*-1)-\alpha\widehat{k}S^*-\gamma\widehat{k}I^*\right].
\end{aligned} \tag{16}$$

When $(((2\beta-\alpha-\gamma)\widehat{k}I^*+(\alpha+\beta)\widehat{k}S^*)/(\beta\widehat{k}+\lambda_1+\lambda_2+\widetilde{\lambda}_3+\varepsilon)) < 1$, we can deduce that $c_1 > 0$ and $c_2 > 0$. Based on the Routh–Hurwitz criteria, the equilibrium point $E_3 = (S^*, I^*)$ is asymptotically stable if $(((2\beta-\alpha-\gamma)\widehat{k}I^*+(\alpha+\beta)\widehat{k}S^*)/(\beta\widehat{k}+\lambda_1+\lambda_2+\widetilde{\lambda}_3+\varepsilon)) < 1$. □

4. Numerical and Simulation Analysis

4.1. Dynamic Simulation of Panic Diffusion with Guidance. In this part, a dynamic panic propagation model of subway passengers with guidance strategies is established, which is

based on the SIR model of differential equations in Section 3. There are $N = 1400$ passengers in the subway car. We set the model parameters as the length and width of the subway car, which is consistent with reference [3]. Considering the off-peak hours, the number of people in the subway cars has not reached the peak, and they are not crowded. Therefore, the degree of the small-world network describing the social group was used to define the intergroup in the simulation of the dynamic contagion model, as given by equations (1)–(3), where $\widehat{k} = 2.5$.

The initial susceptible and infected proportions are $S(t) = 0.9$ and $I(t) = 0.1$, respectively. Once danger breaks out in a confined space, people's panic spreads very fast. Therefore, the infection rate is set as $\beta = 0.4$. Calm people are susceptible to becoming infected if there are infections around them. Therefore, we can use the immune loss rate to represent the possibility of changing because of the circumstances. Furthermore, we set the infection rate as $\alpha = 0.1$, the immune loss rate as $\gamma = 0.04$, and the trust parameters as $\lambda_1 = 0.001$, $\lambda_2 = 0.7$, $\widetilde{\lambda}_3 = 0.1$, and $\varepsilon = 0$. Figure 2 shows the results of solving the dynamic differential equations equations (1)–(3) in MATLAB 2014a.

At this point, the steady ratio of the three groups is $E_1 = (1, 0, 0)$. According to all the parameters, the stability conditions are calculated as $\alpha\widehat{k}/(\varepsilon + \lambda_2) = 0.3571 < 1$. Therefore, Theorem 1 is proved.

Then, Figure 3 shows the results of changing all the parameters to satisfy $0 < (((\alpha + \beta)\widehat{k} \cdot \widetilde{\lambda}_3)/((\beta\widehat{k} + \varepsilon + \lambda_2) \cdot (\lambda_1 + \widetilde{\lambda}_3))) < 1$, where $\alpha = 0.9$, $\beta = 0.1$, $\gamma = 0.1$, $\lambda_1 = 0.5$, $\lambda_2 = 0.3$, $\widetilde{\lambda}_3 = 0.1$, and $\varepsilon = 0$. From the simulation results, we find that the equilibrium solution is $(0.1677, 0, 0.8377)$. We can calculate $S^* = \widetilde{\lambda}_3/(\lambda_1 + \widetilde{\lambda}_3) = 1/6 \approx 0.1667$, $R^* = \lambda_1/(\lambda_1 + \widetilde{\lambda}_3) = 5/6 \approx 0.8337$, and $(((\alpha + \beta)\,\widehat{k} \cdot \widetilde{\lambda}_3)/((\beta\,\widehat{k} + \varepsilon + \lambda_2) \cdot (\lambda_1 + \widetilde{\lambda}_3))) = (((0.9 + 0.1) \times 2.5 \times 0.1)/((0.1 \times 2.5 + 0 + 0.3) \times 0.6)) < 1$.

The simulation results are consistent with the theoretical results, which prove that Theorem 2 is correct.

We have performed several groups of experiments and compared the simulation data results with the theoretical analysis results to verify the correctness of Theorem 2. Due to space limitations, only 10 sets of data are shown in Table 1. These data are obtained by changing the different trust parameters when $\alpha = 0.9$, $\beta = 0.4$, and $\gamma = 0.3$. The values of columns 5–7 in Table 1 are the simulation results. The values of columns 8–11 are the theoretical calculation results. From Table 1, we set $\sigma_1 = \alpha\widehat{k}/(\varepsilon + \lambda_2)$ and $\sigma_2 = ((\alpha + \beta)\widehat{k} \cdot \widetilde{\lambda}_3)/((\beta\widehat{k} + \varepsilon + \lambda_2) \cdot (\lambda_1 + \widetilde{\lambda}_3))$. It can be seen from the comparison results that the simulation results are equal to the disease-free equilibrium point of differential equations (1)–(3) with $\sigma_1 > 1$ and $\sigma_2 < 1$.

To verify Theorem 3, we change the value of the trust parameter sets $(\lambda_1, \lambda_2, \widetilde{\lambda}_3)$, and the simulation results are shown as Figure 4. From this simulation, the dynamic proportions of the three groups at the endemic equilibrium $E_3 = (S^*, I^*, R^*) = (0.2151, 0.5395, 0.2454)$. At this time, the conditions of Theorem 3 are verified by calculating equations (17)–(19).

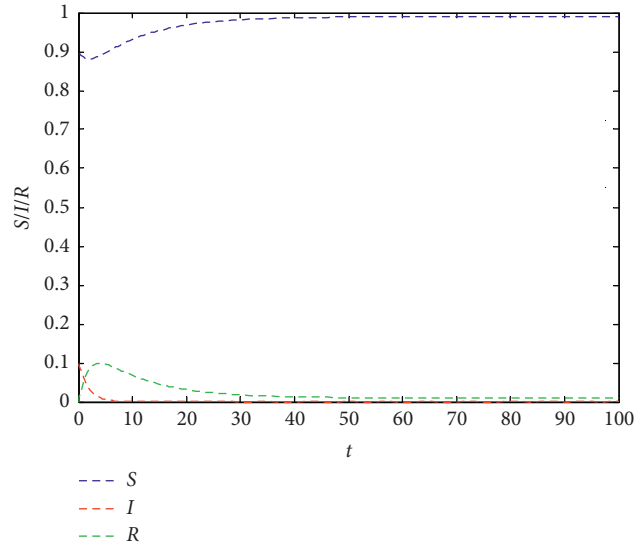

Figure 2: The dynamic proportions of the three groups over time. ($\alpha = 0.1, \beta = 0.4, \gamma = 0.04, \lambda_1 = 0.001, \lambda_2 = 0.7, \widetilde{\lambda}_3 = 0.1$, and $\varepsilon = 0$).

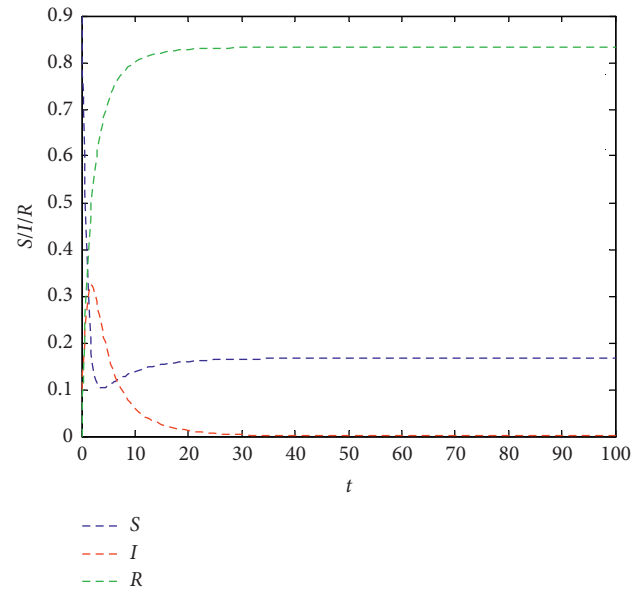

Figure 3: The dynamic proportions of the three groups over time with ($\alpha = 0.9$, $\beta = 0.1$, $\gamma = 0.1$, $\lambda_1 = 0.5$, $\lambda_2 = 0.3$, $\widetilde{\lambda}_3 = 0.1$, and $\varepsilon = 0$).

$$\varphi_1 = \frac{\alpha\widehat{k}}{\varepsilon + \lambda_2} = \frac{0.9 * 2.5}{0.3} = 7.5 > 1, \tag{17}$$

$$\varphi_2 = \frac{(\alpha + \beta)\widehat{k}}{\beta\widehat{k} + \varepsilon + \lambda_2} = \frac{(0.9 + 0.3) * 2.5}{0.3 * 2.5 + 0.3} = 2.8571 > 1, \tag{18}$$

$$\varphi_3 = \frac{(2\beta - \alpha - \gamma)\widehat{k}I^* + (\alpha + \beta)\widehat{k}S^*}{\beta\widehat{k} + \lambda_1 + \lambda_2 + \widetilde{\lambda}_3 + \varepsilon} < 1. \tag{19}$$

We conducted 500 simulation experiments by the transforming parameters, and we selected some of these results, which are presented in Tables 2 and 3. It can be seen

Table 1: The simulation results and theoretical results at E_2.

	λ_1	λ_2	$\widetilde{\lambda}_3$	S^*	I^*	R^*	σ_1	σ_2	$\widetilde{\lambda}_3/(\lambda_1+\widetilde{\lambda}_3)$	$\lambda_1/(\lambda_1+\widetilde{\lambda}_3)$
1	0.15	0.30	0.01	0.0625	0.0000	0.9375	0.4212	0.4400	0.0100	0.0625
2	0.15	0.30	0.05	0.2500	0.0000	0.7500	0.4275	0.4000	0.0500	0.2500
3	0.30	0.30	0.1	0.2500	0.0000	0.7500	0.3386	0.5000	0.1000	0.2500
4	0.7	0.30	0.1	0.1250	0.0000	0.8750	0.2131	0.9000	0.1000	0.1250
5	0.7	0.3	0.2	0.2222	0.0000	0.7778	1.2131	0.8000	0.2000	0.2222
6	0.9	0.5	0.3	0.2500	0.0000	0.7500	3.2131	1.1000	0.3000	0.2500
7	0.7	0.5	0.3	0.3000	0.0000	0.7000	4.2131	0.9000	0.3000	0.3000
8	0.7	0.3	0.4	0.3637	0.0000	0.6363	5.2131	0.6000	0.4000	0.3636
9	0.8	0.3	0.5	0.3846	0.0000	0.6154	6.2131	0.6000	0.5000	0.3846
10	0.9	0.4	0.2	0.1818	0.0000	0.8182	2.2131	1.1000	0.2000	0.1818

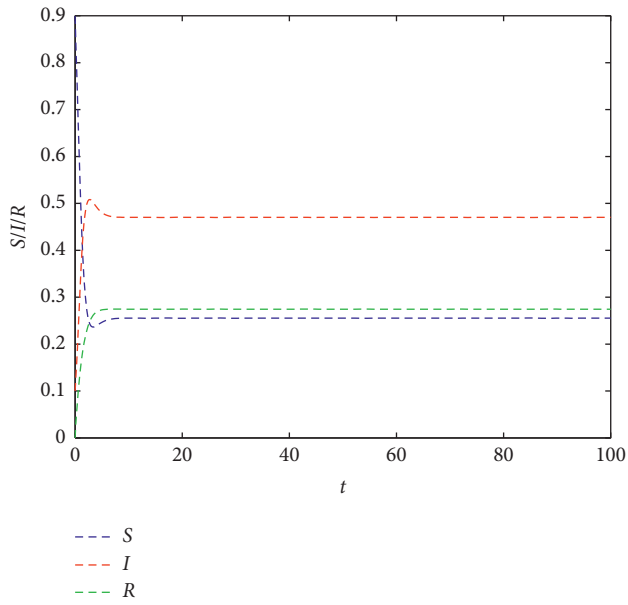

Figure 4: The dynamic proportions of the three groups over time with ($\alpha = 0.9$, $\beta = 0.4$, $\gamma = 0.4$, $\lambda_1 = 0.2$, $\lambda_2 = 0.3$, $\widetilde{\lambda}_3 = 0.7$, and $\varepsilon = 0$).

that the dynamic differential equation has an endemic equilibrium, when $\alpha\widehat{k}/(\varepsilon+\lambda_2) > 1$, $(((\alpha+\beta)\widehat{k})/(\beta\widehat{k}+\varepsilon+\lambda_2)) > 1$, and $((2\beta-\alpha-\gamma)\widehat{k}I^* + (\alpha+\beta)\widehat{k}S^*/(\beta\widehat{k}+\lambda_1+\lambda_2+\widetilde{\lambda}_3+\varepsilon)) < 1$. At present, there are feasible solutions for equation (15), and all solutions have negative real parts that meet the Routh–Hurwitz criteria.

4.2. The Dynamic Analysis of Panic Diffusion with Changing Parameters. In this section, we need to discuss two aspects: one is the influencing factors of the emotional transmission in infected groups by numerically analyzing the simulation results, and the other is the dynamic change of panic diffusion with guidance. When the trust parameters are relatively small, for example, $\lambda_1 = 0.05$, $\lambda_2 = 0.03$, and $\widetilde{\lambda}_3 = 0.01$, an approximation of the low-trust scenario without guidance is obtained. Then, the high-trust scenario is obtained when the trust parameters are set to $\lambda_1 = 0.5$, $\lambda_2 = 0.3$, and $\widetilde{\lambda}_3 = 0.1$. Because the guidance information calms the panic, the proportion of the potentially infected group that transitions directly into the immune group is 0.5. When accepting the guidance, the proportion of the infected group that changes to the immune group is 0.3. The proportion of the immune group that changes to the potentially infected group is 0.1 due to the loss of trust in the guidance.

First, the change in the rate of infected people due to the change of α is shown in Figures 5 and 6. According to reference [2], the probability of infected persons becoming immune is generally higher than that of immune persons becoming susceptible, and we set $\beta = 0.4$ and $\gamma = 0.1$. As seen from Figures 5 and 6, no matter what the trust situation is, the higher infection rate will inevitably lead to a greater increase in the rate of infected people. In Figure 5, in the absence of guidance information, the higher the proportion of the infected group is, the higher the panic in the system. After reaching the peak, the larger the α is, the faster the group panic in the system will calm down. Compared with a small value of α, it can be considered that this situation tends to stabilize rapidly, which is due to the self-organizing behavior in the group. When an emergency occurs and people feel threatened, they will quickly move towards other groups. A small α can be interpreted as a small proportion of potentially infected people being infected. In other words, the potentially infected group is not affected by the panicked groups around them and is isolated from the panic of others. Leaders in general have these qualities. Of course, since the factors that are affected by the surrounding environment are relatively small, the emotional recovery time is slower than that of α. The conclusion is consistent with reference [2].

As shown in Figure 6, in the case of high trust, the infection proportion peaked at 0.25 when the infection rate was high. Different from the situation that is shown in Figure 5, the calm time of people with high infection rates is higher than that of people with low infection rates. It reflects that when following the guidance, the crowd receives the guiding information, gradually tends to calm down, and the self-organizing behavior is not obvious.

We change the external-immunization rate β that represents the rate at which the infected group changes to the calm group over time t due to the panic attenuation around calm group. The results of different trust situations are presented in Figures 7 and 8. In either case, it is obvious that the higher the autoimmune rate is, the smaller the proportion of infected people. We can see that the infected group is affected by the environment and experienced a reduced rate of panic. A higher β indicates that the infected group has a higher acceptance of the environment, and it is

Table 2: The simulation results and theoretical results at E_3 ($\alpha = 0.9$, $\beta = 0.3$, and $\gamma = 0.02$).

	λ_1	λ_2	$\widetilde{\lambda}_3$	S^*	I^*	R^*	φ_1	φ_2	φ_3	c_1	c_2
1	0.02	0.01	0.01	0.2522	0.0045	0.7433	225.00	1.3158	0.9537	0.0072	0.0370
2	0.01	0.02	0.01	0.2545	0.0090	0.7365	112.50	1.9481	0.9584	0.0140	0.0238
3	0.01	0.03	0.01	0.2577	0.0087	0.7336	75.00	1.9231	0.9586	0.0135	0.0140
4	0.01	0.04	0.01	0.2610	0.0085	0.7305	56.25	1.8987	0.9592	0.0129	0.0039
5	0.01	0.2	0.01	0.3200	0.2600	0.4200	11.25	1.5789	0.8020	0.1985	0.0280
6	0.02	0.02	0.01	0.2544	0.0090	0.7367	112.50	1.2987	0.9460	0.0139	0.0341
7	0.02	0.03	0.01	0.2556	0.0043	0.7401	75.00	1.2821	0.9431	0.0065	0.0265
8	0.03	0.03	0.02	0.2568	0.0128	0.7305	75.00	1.5385	0.9173	0.0200	0.0599
9	0.03	0.04	0.02	0.2602	0.0123	0.7275	56.25	1.5190	0.9192	0.0187	0.0491
10	0.03	0.05	0.02	0.2638	0.0118	0.7244	45.00	1.5000	0.9212	0.0175	0.0381
11	0.04	0.03	0.02	0.2580	0.0080	0.7340	75.00	1.2821	0.9147	0.0123	0.0625
12	0.04	0.04	0.02	0.2614	0.0076	0.7310	56.25	1.2658	0.9165	0.0110	0.0518
13	0.04	0.05	0.02	0.2649	0.0071	0.7280	45.00	1.2500	0.9183	0.0096	0.0410
14	0.11	0.11	0.1	0.2707	0.0639	0.6654	20.45	1.6611	0.7172	0.1094	0.2990
15	0.11	0.12	0.1	0.2745	0.0619	0.6636	18.75	1.6420	0.7224	0.1042	0.2860
16	0.11	0.14	0.1	0.2821	0.0581	0.6598	16.07	1.6051	0.7325	0.0941	0.2600
17	0.11	0.2	0.1	0.3047	0.0478	0.6475	11.25	1.5038	0.7591	0.0649	0.1842
18	0.13	0.11	0.1	0.2730	0.0547	0.6723	20.45	1.5167	0.7162	0.0940	0.3049
19	0.13	0.12	0.1	0.2768	0.0527	0.6705	18.75	1.4993	0.7214	0.0885	0.2917
20	0.13	0.15	0.1	0.2882	0.0471	0.6647	15.00	1.4493	0.7359	0.0726	0.2531
21	0.13	0.2	0.1	0.3070	0.0388	0.6542	11.25	1.3730	0.7574	0.0472	0.1901
22	0.21	0.21	0.2	0.2964	0.0937	0.6100	10.71	1.5244	0.6011	0.1866	0.5459
23	0.21	0.25	0.2	0.3128	0.0821	0.6051	9.00	1.4634	0.6247	0.1495	0.4874
24	0.21	0.27	0.2	0.3208	0.0768	0.6024	8.33	1.4347	0.6355	0.1314	0.4589
25	0.23	0.21	0.2	0.2988	0.0850	0.6162	10.71	1.4535	0.6020	0.1695	0.5517
26	0.23	0.23	0.2	0.3069	0.0791	0.6140	9.78	1.4238	0.6136	0.1504	0.5227
27	0.23	0.25	0.2	0.3150	0.0736	0.6115	9.00	1.3953	0.6248	0.1315	0.4939
28	0.25	0.21	0.2	0.3009	0.0764	0.6228	10.71	1.3889	0.6022	0.1527	0.5586
29	0.25	0.23	0.2	0.3090	0.0705	0.6205	9.78	1.3605	0.6138	0.1328	0.5293
30	0.27	0.21	0.2	0.3031	0.0677	0.6292	10.71	1.3298	0.6027	0.1353	0.5649

easier to calm the nervous emotions of the infected group and restrain outward fluctuations. The smaller the β is, the lower the internal panic tolerance of this group is, and the inner vulnerability is manifested as not accepting external calming information and ignoring external information. These two results are consistent with the real situation, indicating that the model can effectively reflect the spread of panic.

Next, the rate of infection varies over time with the different immune loss rates γ, $\alpha = 0.9$ and $\beta = 0.4$, as shown in Figures 9 and 10.

Figure 9 shows that when the immune loss rate is 0.4 and 0.5, the system's panicked population is the largest, and the calm time is the longest under the absence of guidance.

This is an interesting phenomenon, and thus, we qualitatively analyze the reasons. In the case of an emergency without guidance, if the group immunity loss rate is relatively low, the crowd will continue this calm state and no longer produce panic once the crowd enters the calm state. When the population's immunity loss rate is high, the change rate from the calm population (R) to the susceptible population (S) is large, and the system input is large. Since $\alpha = 0.9$, the infection rate of the infected people is also large. As a result, the ratio of the three groups will rapidly shift and eventually level off. When $\gamma = 0.4$ or $\gamma = 0.5$, the system's stationary time is prolonged, and the conversion rate of the three groups is slower. To further analyze this case, the influence of the guidance will be numerically analyzed in Section 4.3.

Figure 10 shows that when the group has a high degree of trust, the immune loss rate γ is small, the proportion of the panicked group is low, and the calm time of the infected group is short. Because there is less immune loss in system, fewer people are moving from the calm groups to potential groups. Therefore, there is less input and less overall panic. In contrast, a larger number indicates a higher rate of movement from the calm group to the susceptible group, a higher rate of system input, and a higher rate of panic. It takes a long time for this dynamic system to calm down.

4.3. The Dynamic Analysis of Panic Diffusion with Changing Multitrust Parameters. From Figures 5–10, in the case of low trust, the peak value of panic is high and close to 0.9. In the case of high trust, the peak value of the panic ratio is below 0.35. It shows that effective organization and guidance can reduce group panic very well. To further analyze the role of guidance, in this part, a comprehensive simulation and analysis of the trust parameter are carried out.

There are three main components of the trust parameter: the rate of susceptibility to being infected with guidance λ_1, the rate of changing from infected to recovered with guidance λ_2, and the guidance loss rate of recovery $\widetilde{\lambda}_3$. In this part, the degree of influence of each parameter on the total

Table 3: The simulation results and theoretical results at E_3 ($\alpha = 0.9$, $\beta = 0.4$, and $\gamma = 0.4$).

	λ_1	λ_2	$\widetilde{\lambda}_3$	S^*	I^*	R^*	σ_1	σ_2	σ_3	c_1	c_2
1	0.1	0.15	0.2	0.1639	0.5444	0.2917	15.00	1.8841	0.6490	0.5812	1.6477
2	0.2	0.2	0.2	0.2243	0.3695	0.4062	11.25	1.3542	0.6288	0.3731	1.3329
3	0.2	0.3	0.6	0.2235	0.5060	0.2705	7.50	1.8750	0.5266	1.8626	2.3060
4	0.3	0.35	0.6	0.2620	0.4185	0.3194	6.43	1.6049	0.5180	1.5524	2.1715
5	0.3	0.35	0.7	0.2521	0.4581	0.2897	6.43	1.6852	0.4949	2.0488	2.4532
6	0.1	0.1	0.6	0.0815	0.8077	0.1109	22.50	2.5325	0.4836	2.9539	3.0448
7	0.2	0.15	0.3	0.2260	0.4156	0.3584	15.00	1.6957	0.6340	0.6776	1.5850
8	0.3	0.3	0.3	0.3556	0.1444	0.5000	7.50	1.2500	0.6653	0.1949	0.9249
9	0.2	0.3	0.4	0.3045	0.3104	0.3851	7.50	1.6667	0.6434	0.6809	1.3985
10	0.2	0.3	0.5	0.2842	0.3763	0.3395	7.50	1.7857	0.6030	1.0996	1.7468
11	0.2	0.3	0.7	0.2553	0.4703	0.2744	7.50	1.9444	0.5374	2.0768	2.3583
12	0.35	0.3	0.5	0.3086	0.2971	0.3943	7.50	1.4706	0.5701	0.8830	1.7185
13	0.35	0.3	0.6	0.2888	0.3619	0.3493	7.50	1.5789	0.5378	1.3520	2.0637
14	0.35	0.3	0.7	0.2887	0.3619	0.3493	7.50	1.6667	0.5148	1.6863	2.2640
15	0.3	0.4	0.4	0.3789	0.1684	0.4526	5.63	1.3265	0.6466	0.3201	1.0791
16	0.3	0.4	0.5	0.3576	0.2377	0.4047	5.63	1.4509	0.6093	0.6626	1.4351
17	0.3	0.4	0.6	0.3405	0.2936	0.3659	5.63	1.5476	0.5768	1.0607	1.7605
18	0.3	0.4	0.7	0.3262	0.3398	0.3340	5.63	1.6250	0.5479	1.5065	2.0647
19	0.1	0.2	0.5	0.2030	0.5403	0.2567	11.25	2.2569	0.5916	1.6117	2.1156
20	0.1	0.2	0.6	0.1895	0.5842	0.2263	11.25	2.3214	0.5547	2.1495	2.4145
21	0.1	0.2	0.7	0.1788	0.6188	0.2024	11.25	2.3698	0.5226	2.7206	2.6924
22	0.5	0.3	0.5	0.3375	0.2031	0.4594	7.50	1.2500	0.5432	0.6569	1.6569
23	0.5	0.3	0.6	0.3123	0.2849	0.4027	7.50	1.3636	0.5120	1.1278	2.0410
24	0.5	0.3	0.7	0.2928	0.3487	0.3585	7.50	1.4583	0.4852	1.6480	2.3844
25	0.2	0.6	0.6	0.4259	0.2161	0.3580	3.75	1.5234	0.6443	0.6696	1.2859
26	0.2	0.6	0.7	0.4150	0.2511	0.3338	3.75	1.5799	0.6149	1.0067	1.5651
27	0.6	0.2	0.6	0.2571	0.3643	0.3786	11.25	1.3542	0.4621	1.4635	2.4196
28	0.6	0.2	0.7	0.2339	0.4400	0.3261	11.25	1.4583	0.4360	2.0799	2.7900
29	0.6	0.6	0.6	0.4882	0.0121	0.4997	3.75	1.0156	0.5699	0.0343	1.2286
30	0.6	0.7	0.7	0.5168	0.0201	0.4631	3.21	1.0294	0.5649	0.0657	1.3455

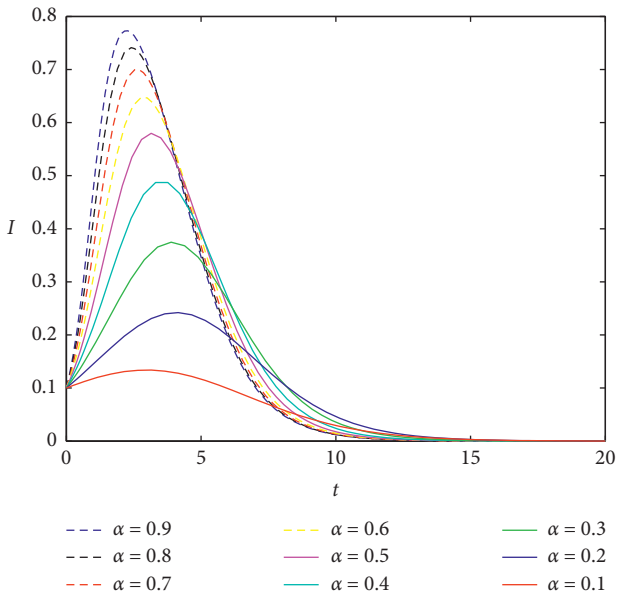

Figure 5: Dynamical proportion of the infected group over time t based on different α values under low trust.

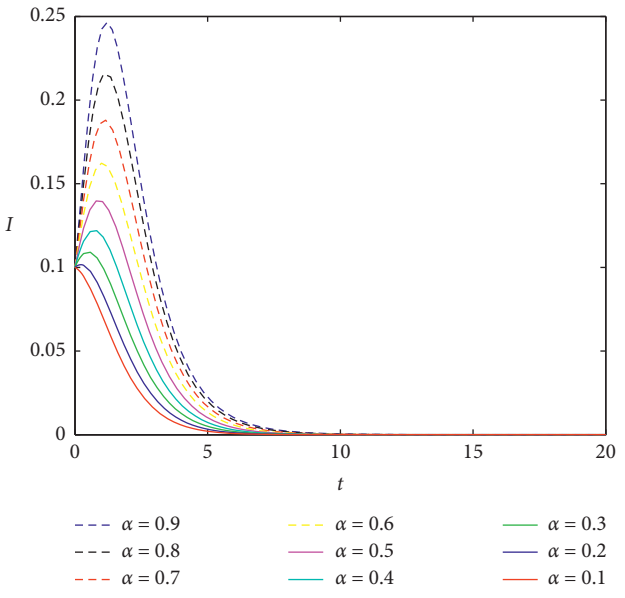

Figure 6: Dynamical proportion of the infected group over time t with different α values under high trust.

panic of the system will be analyzed by using a numerical simulation. The other parameters in the following simulation experiment are set as constant as $\alpha = 0.9$, $\beta = 0.4$, $\gamma = 0.4$, and $\varepsilon = 0$.

We take into account the influence of the proportion of the susceptible group who receive guidance that change to calm on the system panic and set $\lambda_2 = 0.3$, $\widetilde{\lambda}_3 = 0.3$, and $\lambda_1 = 0.1, 0.3, 0.5, 0.7$, as shown in Figure 11. As λ_1 increases,

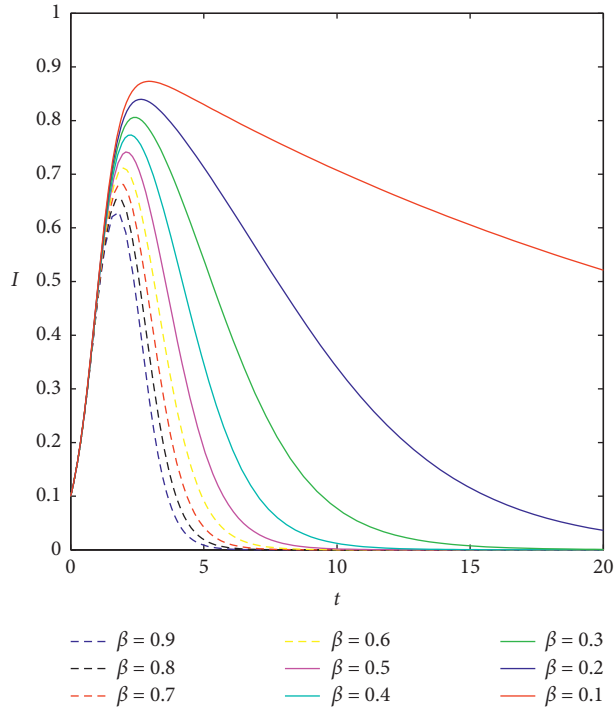

Figure 7: Dynamical proportion of the infected group over time t with different β values under low trust.

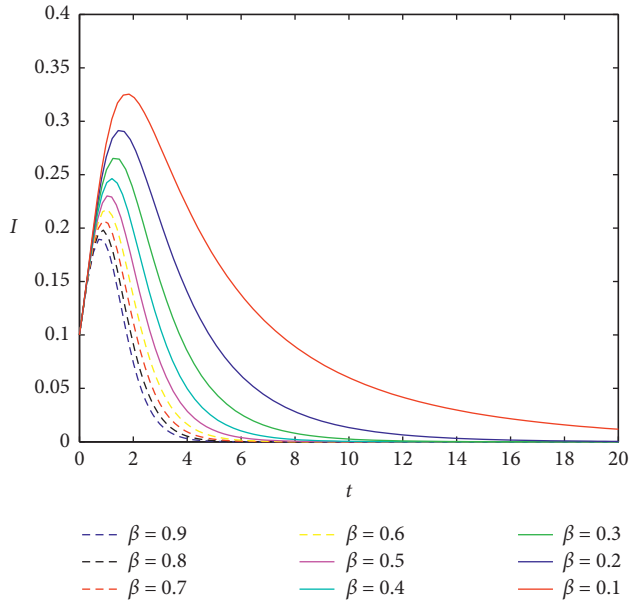

Figure 8: Dynamical proportion of the infected group over time t with different β values under high trust.

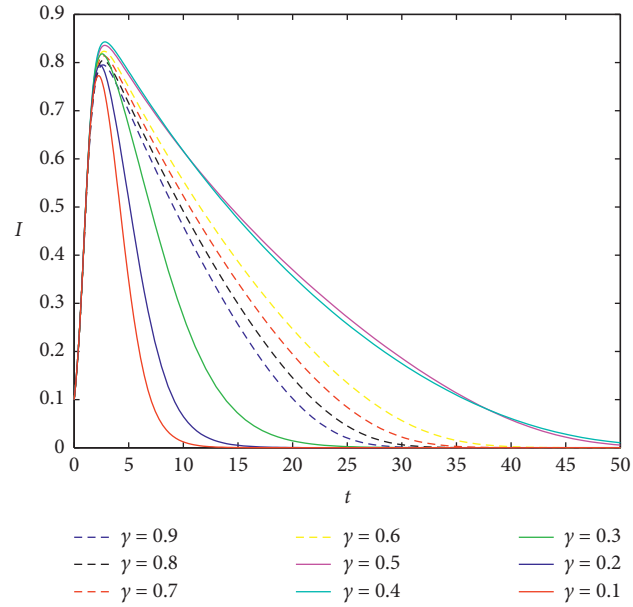

Figure 9: Dynamical proportion of the infected group over time t with different γ values under low trust.

the proportion of infected people in the system decreases. It suggests that though the infection rate is high ($\alpha = 0.9$), the susceptible group who receive official guidance can calm their emotions and change to the calm group to avoid infection. This further explains the importance of official guidance. Subway safety controllers should look for ways to improve people's trust in guidance, especially for those vulnerable to infection to control the panic.

When $\lambda_1 = 0.15$ and $\widetilde{\lambda}_3 = 0.3$, the proportions of the three groups are presented in Figure 12, which shows that the immunity rate gradually increases as $\lambda_2 = 0.1$, 0.2, 0.5, and 0.7. The peak value of the infected group decreases as λ_2 increases in the four situations. Thus, an increase in the proportion of infected people who receive guidance will decrease the systemic panic and avoid the risk of a sudden surge in systemic panic.

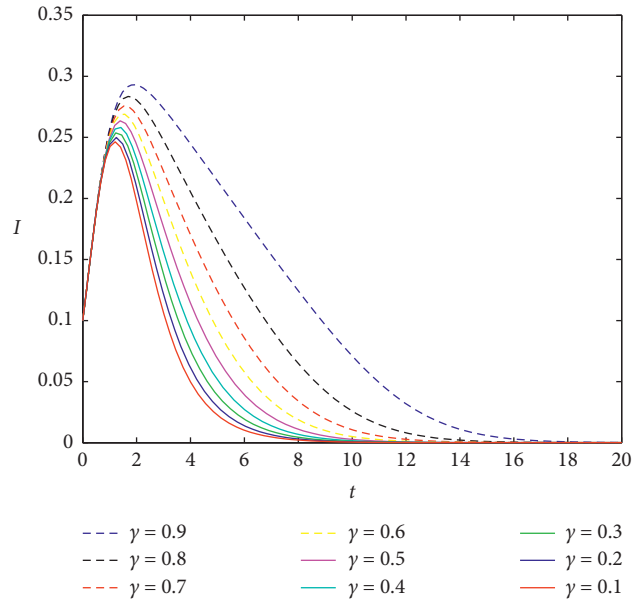

Figure 10: Dynamical proportion of the infected group over time t with different γ values under high trust.

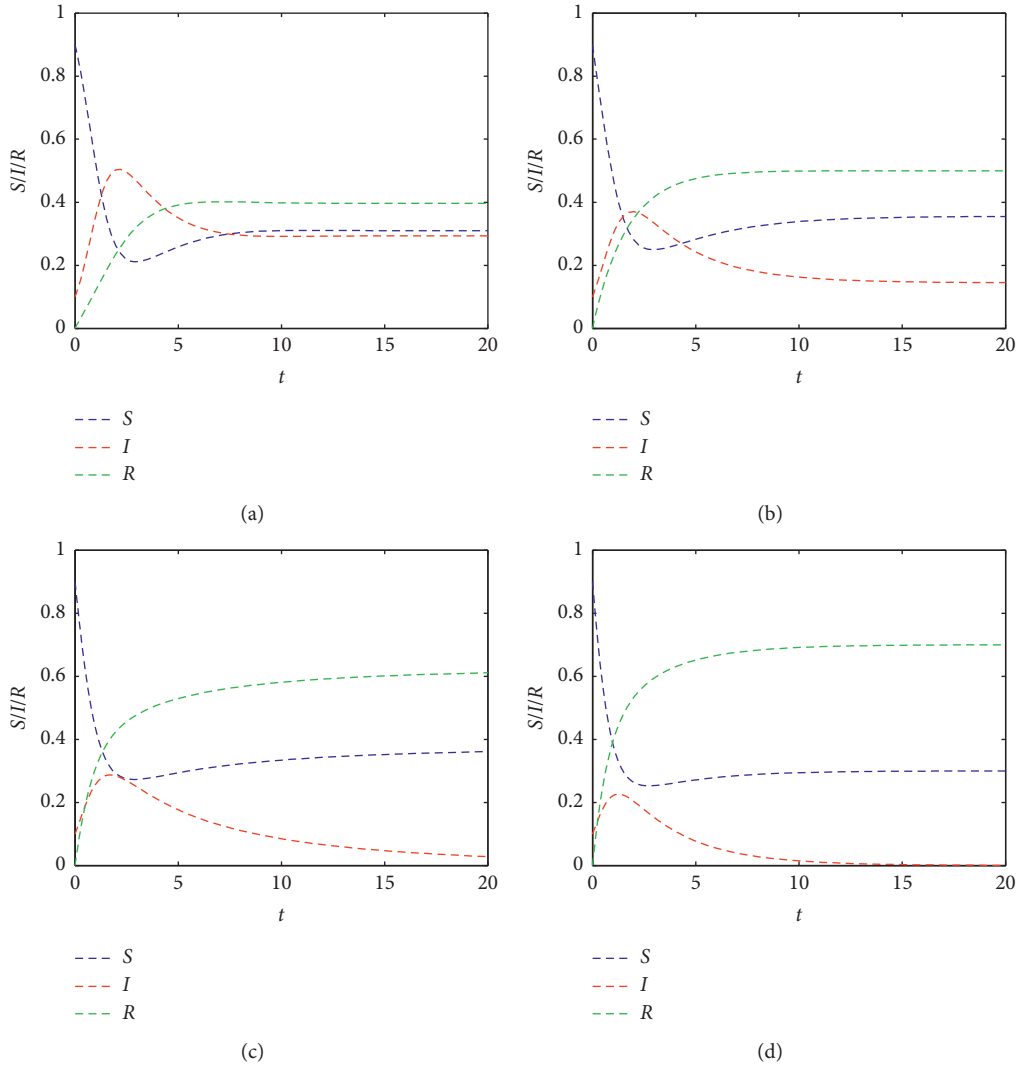

Figure 11: The dynamic proportions of the three groups over time t with different λ_1 values.

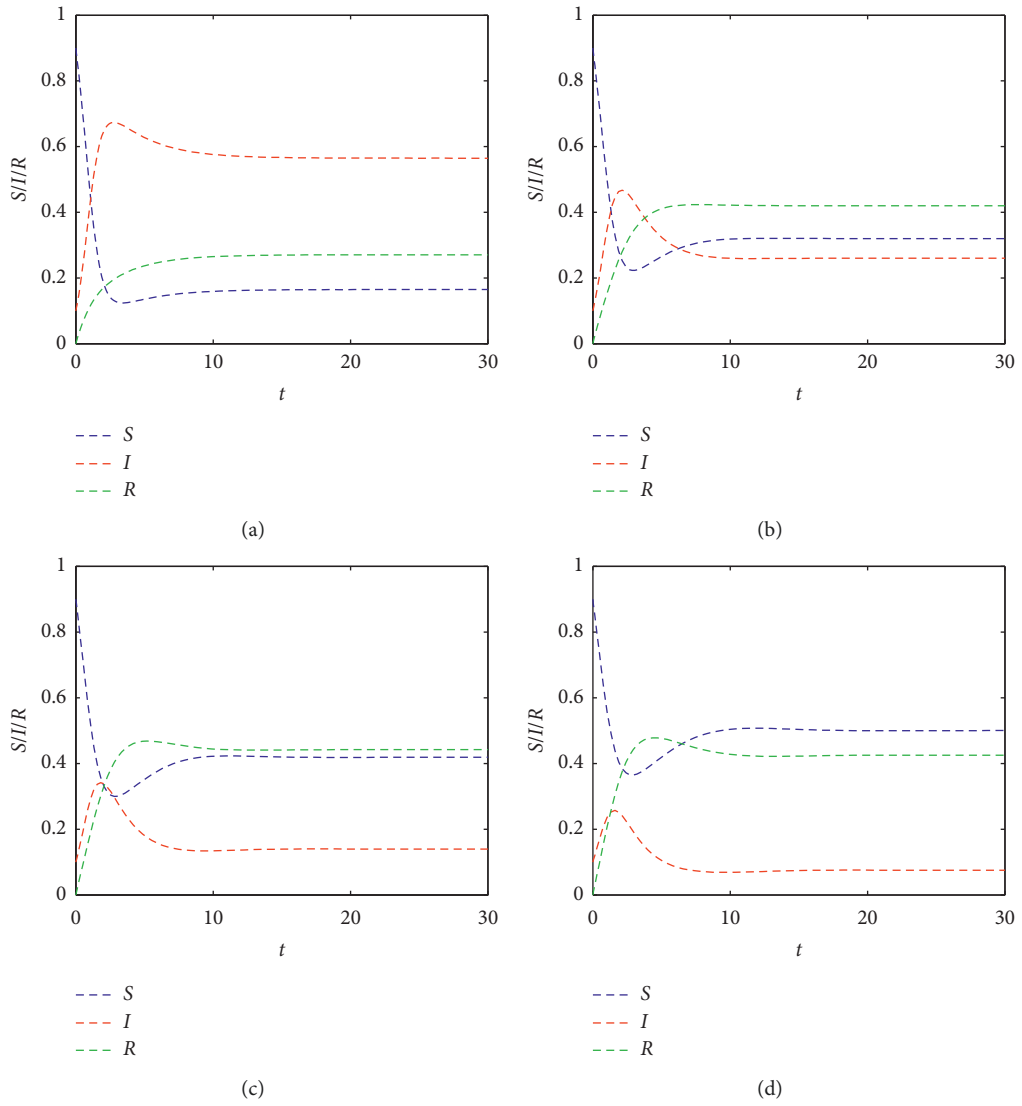

Figure 12: The dynamic proportions of the three groups over time t with different λ_2 values.

The four subplots of Figure 13 are the population proportion plots when $\widetilde{\lambda}_3 = 0.01$, $\widetilde{\lambda}_3 = 0.15$, $\widetilde{\lambda}_3 = 0.3$, and $\widetilde{\lambda}_3 = 0.6$. As seen from the result graphs, the peak infection rates in the four subplots were similar, but the panic rates at the stable points are different. The panic among the population increases with the loss of trust in the guidance.

Figures 11–13 reveal that λ_1 and λ_2 are positively correlated with the proportion of system infection, and $\widetilde{\lambda}_3$ is negatively correlated with the proportion of system infection. Therefore, we set $\theta = \lambda_1 + \lambda_2 - \widetilde{\lambda}_3$ to represent the level of group trust in the system. Figure 14 shows four cases with different levels of trust, and the trust-parameter settings are shown in Table 4. The other parameters are set to $\alpha = 0.9$, $\beta = 0.4$, $\gamma = 0.4$, and $\varepsilon = 0$. I^p represents the peak infection rate. Through simulation experiments, it is found that when $\theta > 0$, the proportion of the panicked group is not more than 0.5. When P hours is reached, the system is calm. A larger θ means that there is a higher level of trust in the whole system and a smaller panicked population.

To analyze the case of $\theta < 0$, four simulation experiments were designed. The experimental parameters and results are shown in Table 5 and Figure 15. From the result of the simulation experiments, the proportion of the panicked group is higher than another groups when $\theta < 0$. In this case of $\theta < 0$, panicked people are the majority. Once there are rumors, there will be the possibility of mass incidents. The loss of trust is so high that the transfer among all kinds of groups to panicked groups occurs, and the amount of panic in the total group remains high. Subway safety controllers must take measures to improve the crowd's trust in the guidance strategy to achieve the purpose of controlling the spread of panic among the crowd.

5. Conclusions

This paper describes a dynamic transmission model of passenger panic in subway cars considering official guidance information. The model combines system dynamics,

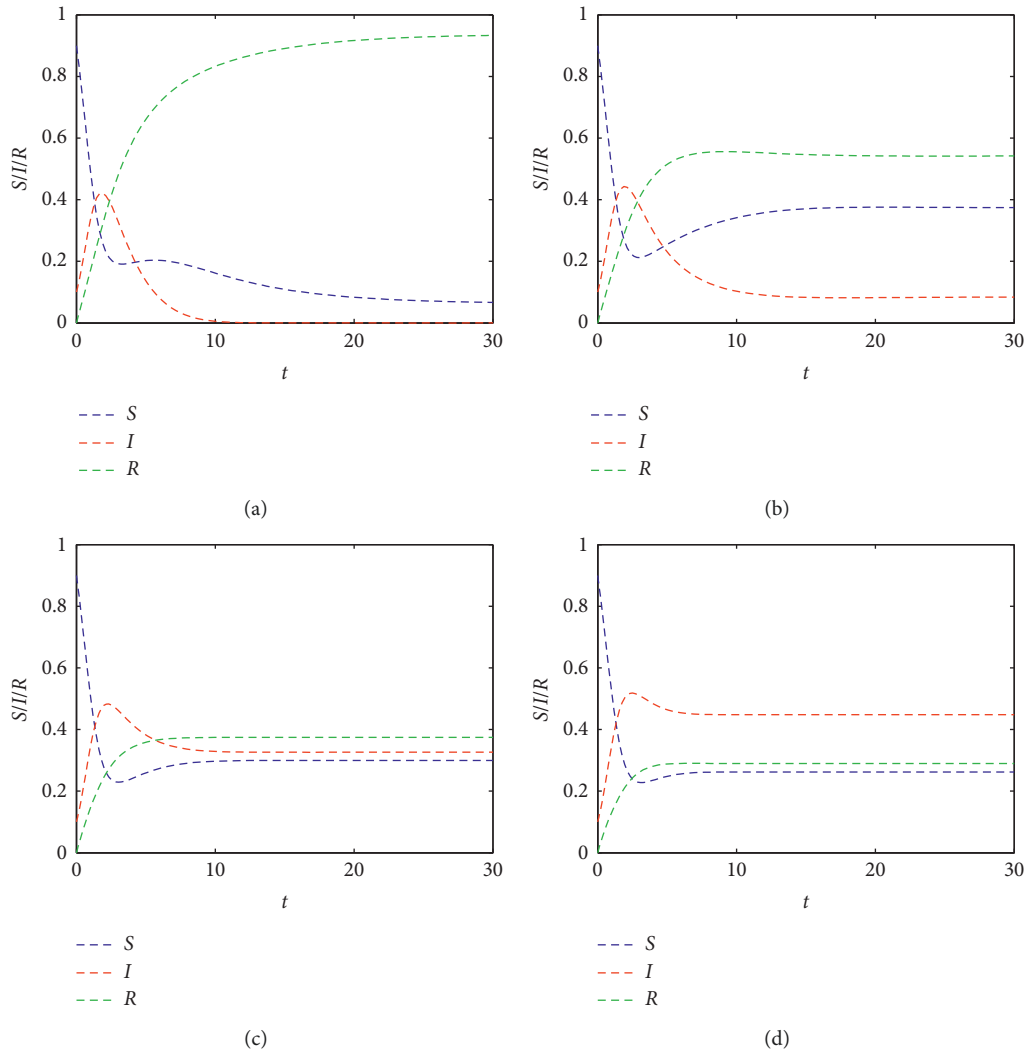

Figure 13: The dynamic proportions of the three groups over time t with different $\widetilde{\lambda}_3$ values.

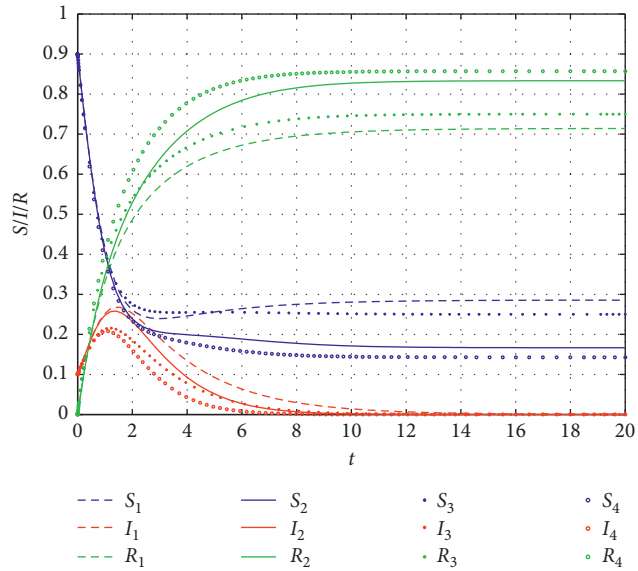

Figure 14: The dynamic proportions of the three groups over time t with different $\theta > 0$.

Table 4: The trust-parameter settings of Figure 14.

	λ_1	λ_2	$\widetilde{\lambda}_3$	S^*	I^*	R^*	θ	I^p
$S_1/I_1/R_1$	0.5	0.3	0.2	0.2857	0	0.7143	0.6	0.2677
$S_2/I_2/R_2$	0.5	0.3	0.1	0.1667	0	0.8333	0.7	0.2582
$S_3/I_3/R_3$	0.6	0.4	0.2	0.2500	0	0.7500	0.8	0.2157
$S_4/I_4/R_4$	0.6	0.4	0.1	0.1429	0	0.8571	0.9	0.2078

Table 5: The trust-parameter settings of Figure 14.

	λ_1	λ_2	$\widetilde{\lambda}_3$	S^*	I^*	R^*	θ	I^p
$S_5/I_5/R_5$	0.1	0.4	0.6	0.3137	0.3804	0.3059	−0.1	0.4709
$S_6/I_6/R_6$	0.2	0.3	0.7	0.2554	0.4702	0.2744	−0.2	0.5070
$S_7/I_7/R_7$	0.2	0.3	0.8	0.2327	0.5433	0.2240	−0.3	0.5520
$S_8/I_8/R_8$	0.3	0.2	0.9	0.1768	0.6253	0.1979	−0.4	0.6253

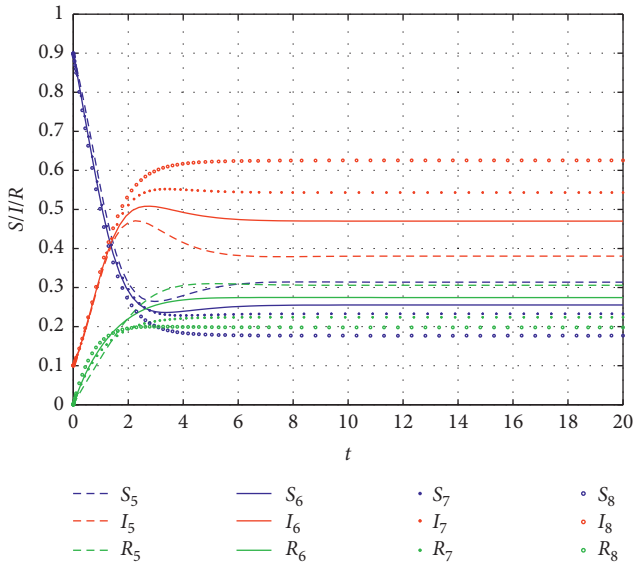

Figure 15: The dynamic proportions of the three groups over time t with different $\theta < 0$.

transmission dynamics, and infectious disease models. By analyzing the evolutionary mechanism of panic of subway passengers during sudden events in subway operations, we provide a method to describe the dynamic spreading model of passenger panic with official guidance information. Through numerical analysis and simulation analysis, it is verified that the model can truly reflect the emotional fluctuations of subway passengers and is effective. This paper provides an effective passenger emotional evolution model for subway safety operation managers, which is helpful for subway operation safety personnel to master the influencing factors of passenger emotions and to carry out effective control strategies.

The innovative points and conclusions of this paper mainly include the following:

(1) This paper creates a trust factor to represent how much passengers trust official information. During emergencies, passengers' emotions are strongly affected by the trust factor θ. In the previous literatures, the trust factor was equivalent to the immune factor and only affected the infected population. However, from the practical point of view, this paper considers that each group of passengers will be affected by the trust factor. Moreover, this paper draws the conclusion that θ is negatively correlated with the steady state of the system. Furthermore, the simulation analysis proves that the official guidance is very necessary in emergencies. The correct information being provided by authorities can effectively control the spread of panic. In addition, it is important to pay attention to the continuous effectiveness of official guidance information in order to maintain a high degree of trust in official information. Once there is a loss of trust, the groups will experience turbulent changes, and the panic among the group will increase, resulting in the intensification of group events.

(2) In this paper, the immune factor is divided into three components: the internal self-recovery ε, the influence of the calm crowd β, and the official guiding factor λ_2. The immune factor is not just a constant; it can be broken down to more finely delineated factors that affect the transition from infected to calm. This breakdown is conducive to clarifying the influence of various factors in the mechanism of emotional transmission and for subway safety operators to effectively control panicked crowds to avoid the formation of large-scale mass panic.

(3) Through the numerical and simulation analysis of the infection model, the influence of each factor on the stability of the system was analyzed. γ is the immune loss rate and reflects the ratio of the calm group to the susceptible group when a calm person contacts an infected group over t. This conclusion reminds subway safety managers that while they are focusing on effectively controlling panic crowds, they should also pay attention to controlling the transition from calm crowds to susceptible ones. In particular, if r is in this region, it may cause system turbulence and increase the panic in the population. Subway safety management departments need to deeply understand the causes of the transformation from calm crowds to susceptible crowds to effectively control mass panic and maintain safety and stability.

Of course, from a microperspective, this paper considers that the emotions of subway passengers that are guided by the authorities can become infected in the carriage, and the total number of passengers is unchanged in this process. Different individual emotions are also not involved, such as the differences in the acceptance factors of men and women that guide trust, the greater sensitivity of women, and other internal microfactors of passengers. The follow-up work will further assess and model the spread of panic among passengers, such as during emergencies when subway vehicles stop at stations and the spreading mechanism of panic among passengers.

Data Availability

The data used to support the findings of this study are available from the corresponding author upon request.

Conflicts of Interest

The authors declare that there are no conflicts of interest regarding the publication of this paper.

Acknowledgments

This work was supported by the Natural Science Foundation of Liaoning Province (grant no. 20170540654), National Natural Science Foundation of China (grant no. 61203152), Program for Liaoning Excellent Talents in University (LNET) (grant no. LJQ2014131), and Natural Science Foundation of Liaoning Province (grant no. 2015020037).

References

[1] Y. Chen, Y. Cai, P. Li, and G. Zhang, "Study on evacuation evaluation in subway fire based on pedestrian simulation technology," *Mathematical Problems in Engineering*, vol. 2015, Article ID 357945, 9 pages, 2015.

[2] T.-C. Yan and M. Yu, "Using the Haddon matrix to explore medical response strategies for terrorist subway bombings," *Military Medical Research*, vol. 6, no. 1, 2019.

[3] H. F. Zhao, J. Jiang, R. Y. Xu et al., "SIRS model of passengers' panic propagation under self-organization circumstance in the subway emergency," *Mathematical Problems in Engineering*, vol. 2014, Article ID 608315, 12 pages, 2014.

[4] C. Li, Y. Pei, M. Zhu, and Y. Deng, "Parameter estimation on a stochastic SIR model with media coverage," *Discrete Dynamics in Nature and Society*, vol. 2018, Article ID 3187807, 7 pages, 2018.

[5] M. Zhou, H. Dong, Y. Zhao, Y. Zhang, and P. A. Ioannou, "Optimal number and location planning of evacuation leader in subway stations," *IFAC-PapersOnLine*, vol. 51, no. 9, pp. 410–415, 2018.

[6] E. Quarantelli, "The behavior of panic participants," *Sociology and Social Research*, vol. 41, no. 3, pp. 187–194, 1957.

[7] A. R. Mawson, "Is the concept of panic useful for study purposes," in *Proceedings of the 2nd International Seminar on Behavior in Fire Emergencies*, National Bureau of Standards, Edinburgh, Scotland, October 1978.

[8] M. Ebihara, A. Ohtsuki, and H. Iwaki, "A model for simulating human behavior during emergency evacuation based on classificatory reasoning and certainty value handling," *Computer-Aided Civil and Infrastructure Engineering*, vol. 7, no. 1, pp. 63–71, 1992.

[9] D. J. Low, "Following the crowd," *Nature*, vol. 407, no. 6803, pp. 465-466, 2000.

[10] B. E. Aguirre, "Emergency evacuations, panic, and social psychology," *Psychiatry: Interpersonal and Biological Processes*, vol. 68, no. 2, pp. 121–129, 2005.

[11] C. X. Wang, X. Suo, S. R. Lyu et al., "Research on panic degree model of emergency evacuation from subway," *China Safety Science Journal*, vol. 25, no. 2, pp. 171–176, 2015.

[12] T. Yu, "Evacuation entropy particle swarms optimization (E-PSO) evacuation model considering panic factors," in *Proceedings of the 2018 IEEE 4th International Conference on Control Science and Systems Engineering (ICCSSE)*, Wuhan, China, August 2018.

[13] H. Yu, Y. M. Wang, P. Y. Qiu, and J. Chen, "Analysis of natural and man-made accidents happened in subway stations and trains: based on statistics of accident cases," *MATEC Web of Conferences*, vol. 272, p. 10, 2019.

[14] A. Eren Başak, U. Güdükbay, and F. Durupınar, "Using real life incidents for creating realistic virtual crowds with data-driven emotion contagion," *Computers & Graphics*, vol. 72, pp. 70–81, 2018.

[15] J.-T. Yang, "Safety risk analysis and countermeasures study on regular mass passenger flow of China's urban subway," *Procedia Engineering*, vol. 135, pp. 175–179, 2016.

[16] C. Liang, C. Yang, J. You, G. Fu, and W. Jiang, "Behavior and psychology of Daegu subway fire accident in Korea," in *Proceedings of the 2017 International Conference on Management Science and Management Innovation (MSMI 2017)*, Wuhan, China, April 2017.

[17] Y. Y. Wang, L. H. Cheng, and S. Li, "Study on the influence of subway passengers' non-adaptive behavior based on knowledge-attitude-practice theory," in *Proceedings of the 2019 International Conference on Intelligent Transportation, Big Data & Smart City (ICITBS)*, Changsha, China, January 2019.

[18] J. Wang, W. Yan, H. Xu, Y. Zhi, Z. Wang, and J. Jiang, "Investigation of the probability of a safe evacuation to succeed in subway fire emergencies based on Bayesian theory," *KSCE Journal of Civil Engineering*, vol. 22, no. 3, pp. 877–886, 2018.

[19] L. Hong, J. Gao, and W. Zhu, "Self-evacuation modelling and simulation of passengers in metro stations," *Safety Science*, vol. 110, pp. 127–133, 2018.

[20] L. Zhang, X. Wu, M. Liu, W. Liu, and B. Ashuri, "Discovering worst fire scenarios in subway stations: a simulation approach," *Automation in Construction*, vol. 99, pp. 183–196, 2019.

[21] Y. Mao, Z. N. Li, and W. He, "Emotion-based diversity crowd behavior simulation in public emergency," *The Visual Computer*, vol. 35, pp. 1–15, 2018.

[22] J. F. Li, "An investigation of pedestrian traffic flow in a representative commercial area in China," *Safety and Reliability*, vol. 38, no. 3, pp. 171–181, 2018.

[23] L. Sun, W. Luo, L. Yao, S. Qiu, and J. Rong, "A comparative study of funnel shape bottlenecks in subway stations," *Transportation Research Part A: Policy and Practice*, vol. 98, pp. 14–27, 2017.

[24] P.-Y. Li, M.-C. Zheng, and H. Hibino, "Map design in subway stations through passengers' wayfinding behavior perspective," *Asian Journal of Environment-Behaviour Studies*, vol. 2, no. 2, pp. 105–115, 2017.

[25] Y. Huang, J. Lei, and K. Wang, "The influence of obstructions of evacuation node on subway stations fire evacuation capability," in *Proceedings of the 8th Annual Meeting of Risk Analysis Council of China Association for Disaster Prevention (RAC 2018)*, Xi'an, China, October 2018.

[26] X. Y. Song, Y. Pan, J. C. Jiang, F. Wu, and Y. J. Ding, "Numerical investigation on the evacuation of passengers in metro train fire," *Procedia Engineering*, vol. 211, pp. 644–650, 2018.

[27] S. Cao, W. Song, and W. Lv, "Modeling pedestrian evacuation with guiders based on a multi-grid model," *Physics Letters A*, vol. 380, no. 4, pp. 540–547, 2016.

[28] X. Y. Liu, C. Liu, and X. P. Zeng, "Online social network emergency public event information propagation and

nonlinear mathematical modeling," *Complexity*, vol. 2017, Article ID 5857372, 7 pages, 2017.

[29] D. Xu, X. Xu, Y. Xie, and C. Yang, "Optimal control of an SIVRS epidemic spreading model with virus variation based on complex networks," *Communications in Nonlinear Science and Numerical Simulation*, vol. 48, pp. 200–210, 2017.

[30] L. Zhang, C. Su, Y. Jin, M. Goh, and Z. Wu, "Cross-network dissemination model of public opinion in coupled networks," *Information Sciences*, vol. 451-452, pp. 240–252, 2018.

[31] L. A. Huo, L. Wang, N. Song, C. Ma, and B. He, "Rumor spreading model considering the activity of spreaders in the homogeneous network," *Physica A: Statistical Mechanics and Its Applications*, vol. 468, pp. 855–865, 2017.

[32] R. Li, W. Wang, and Z. Di, "Effects of human dynamics on epidemic spreading in Côte d'Ivoire," *Physica A: Statistical Mechanics and Its Applications*, vol. 467, pp. 30–40, 2017.

[33] J. Q. Kan and H. F. Zhang, "Effects of awareness diffusion and self-initiated awareness behavior on epidemic spreading—an approach based on multiplex networks," *Communications in Nonlinear Science and Numerical Simulation*, vol. 44, pp. 193–203, 2015.

[34] L. Zhu and Y. Wang, "Rumor spreading model with noise interference in complex social networks," *Physica A: Statistical Mechanics and Its Applications*, vol. 469, pp. 750–760, 2017.

[35] H. Zang, "The effects of global awareness on the spreading of epidemics in multiplex networks," *Physica A: Statistical Mechanics and Its Applications*, vol. 492, pp. 1495–1506, 2018.

[36] P. Jiang and X. B. Yan, "Stability analysis and control models for rumor spreading in online social networks," *International Journal of Modern Physics C*, vol. 28, no. 5, Article ID 1750061, 2017.